EVOLUTION OF THE ELECTRIC POTENTIAL AND TURBULENCE IN OH AND ECRH LOW-DENSITY PLASMAS AT THE T-10 TOKAMAK

A.V. MELNIKOV [1,2]
[1] National Research Centre 'Kurchatov Institute',
[2] National Research Nuclear University 'MEPhI',
115409 Moscow, Russian Federation
Email: Melnikov_AV@nrcki.ru

L.G. ELISEEV, S.A. GRASHIN, M.A. DRABINSKIY, P.O. KHABANOV, N.K. KHARCHEV, V.A. KRUPIN, S.E. LYSENKO, A.R. NEMETS, M.R. NURGALIEV, D.A. RYZHAKOV, R.V. SHURYGIN, N.A. SOLOVIEV, V.A. VERSHKOV and T-10 TEAM
National Research Centre 'Kurchatov Institute'
123182 Moscow, Russian Federation

Abstract

Plasma regime with a positive core electric potential (positive electric field) was obtained for the first time in a tokamak. This low-collisionality regime was reached by strong electron-cyclotron resonance heating (P_{EC} = 2.2 MW) of the low-density ($\bar{n}_e \sim 1.0\times10^{19}$ m^{-3}) plasmas in the T-10 circular tokamak (B_0=2.2 T, R=1.5 m, a=0.3 m, I_{pl} = 230 kA). The obtained positive electric field is not consistent with NC approach and suggests turbulence origins. The coupling of plasma potential and collisionality was extended towards the 'banana' collisional regime predicted for ITER, so the positive plasma potential is expected for ITER plasmas.

1. INTRODUCTION

The direct measurement of the electric potential φ in the core of magnetically confined thermonuclear toroidal plasmas is of a paramount importance for the understanding of the role of the radial electric field $E_r = -d\varphi/dr$ for plasma transport and confinement. However, to measure directly E_r or plasma potential φ is a challenging task in the fusion research since the capabilities of the present diagnostics are limited to the plasma edge, like probes, or peripheral areas like reflectometry, and their capabilities to measure E_r or φ are based on some assumptions, which are not always working. A unique diagnostic to study directly plasma potential is Heavy Ion Beam Probe (HIBP). In the past, tokamak plasmas were always characterized by a negative core plasma electric potential [1]. An increase in the plasma density n_e obtained by gas puff results in a more negative plasma potential. An increase in the plasma electron temperature T_e due to the auxiliary heating results in a less negative plasma potential. This is valid for both the steady-state and initial phases of the discharge with plasma current and density ramp. These observations are in a qualitative consistence with neoclassical (NC) theory of plasma energy and particle transport, which is based on the Coulomb collisions of the plasma particles in the presence of magnetic field [2].

Unification of the above tendencies lead to an establishment of the link of plasma potential to plasma effective collisionality, $\nu_{eff} \sim n_e/T_e^2$: the higher is the collisionality, the lower is plasma potential, or the stronger is the negative radial electric field [1]. In stellarators the similar tendency also takes place: the higher density (collisionality) plasmas are characterized by stronger negative plasma potential [3]. On top of that, in low-density (collisionality) stellarator plasmas the core plasma potential has a positive sign [4, 5], which have never been observed in a tokamak.

This paper is dedicated to the reaching of the low-collisionality plasma regime with positive electric potential in a tokamak and an experimental study of the coupling between the plasma potential and collisionality up to its reactor-scale values.

2. EXPERIMENTAL SETUP

The study was performed on the T-10 tokamak (circular tokamak, B_0 = 1.7–2.42 T, R = 1.5 m, a = 0.3 m). Unique features of the T-10 tokamak are: (1) an electron cyclotron heating (ECRH) with a power P_{EC} of up to 2.2 MW; (2) a complex of diagnostics, including heavy ion beam probing (HIBP), Charge eXchange Recombination Spectroscopy (CXRS) and passive spectroscopy, probe diagnostics of edge plasma and SOL;

HIBP diagnostic measures the plasma potential φ with high spatial (< 1 cm) and temporal (1 μs) resolution. Tl^+ ions with energies E_b up to 330 keV were used to probe the plasma from the edge to the core [6]. Aiming for the extension of the investigation area in plasma towards the central area of the plasma column the HIBP accelerating voltage was recently increased up to 330 kV, which is a record: the maximal voltage ever achieved for the open-air accelerator installed in the fusion devices [7, 8].

The shot-to-shot variation of HIBP probing beam energy E_b from 180 keV to 330 keV, and periodic variation of injection angle by scan of voltage on steering plates (U_{scan}), allow us to measure the plasma potential profile in a wide radial range $0.3 \le \rho = r/a \le 1$. The 5-slits energy analyzer allows us to simultaneously measure fluctuations of the potential and plasma density (using the secondary beam current I_{tot}) with frequencies up to 250 kHz at five sample volumes (SV) in the plasma core ($0.08\,\text{m} < r < 0.3$ m). To study the poloidal correlations and rotation, we used the information obtained with the poloidal displacement of the SVs. The displacement of SVs is varied from 5 to 25 mm.

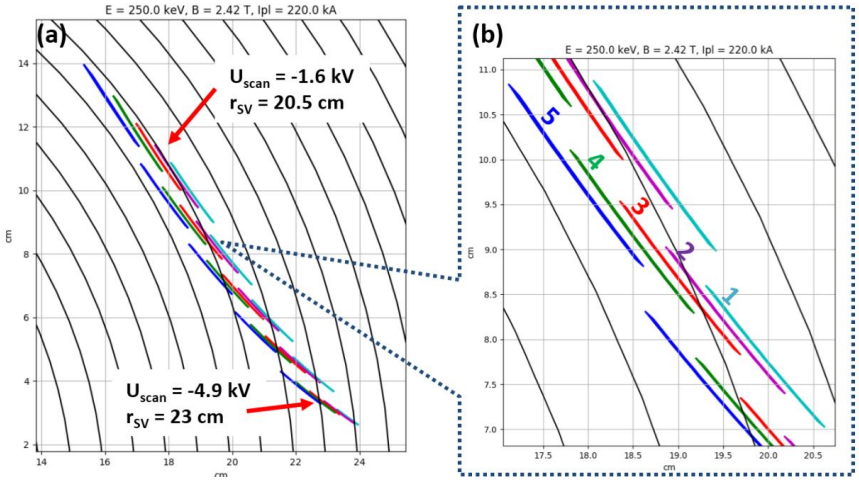

FIG. 1. Positions of sample volumes of a 5-slit analyzer for measuring the poloidal rotation velocity. Probing beam energy E_b = 250 keV, B_t = 2.42 T, I_{pl} = 220 kA.

CXRS measures the profiles of the ion temperature $T_i(r)$, the density of nuclei of light impurities (Li, C, N, O) $n_z(r)$, and toroidal rotation, using a diagnostic neutral hydrogen beam with energy of 30 keV. The measurements were carried out in 9 spatial channels. Measurements of the effective plasma charge $Z_{eff}(r)$ were performed using spectroscopic diagnostics, which measures the spatial profiles of bremsstrahlung radiation in the visible spectral region. The electron density profiles $n_e(r)$ were measured with a 16-channel interferometer. The electron temperature profiles $T_e(r)$ were measured using 24-channel second harmonic electron cyclotron emission (2ω-ECE) from the plasma. The absolute values of the central electron temperature $T_e(0)$ were determined from the spectrum of soft X-ray radiation (SXR).

3. EXPERIMENTAL RESULTS

To obtain the lowest achievable collisionality the auxiliary electron-cyclotron heating (ECRH) was used to heat the ohmic plasma. As ECRH heats plasma electrons, it mimics the power deposition to electrons by fusion alphas in a future fusion reactor. To maximize the HIBP observation area in plasma for Tl^+ beam with achieved energy of 330 keV, the toroidal magnetic field at the axis B_0 should be reduced to B_0 = 1.9 T. However, the most efficient ECR-heating is on-axis, for B_0 = 2.42 T. The compromise allowing the efficient use of ECRH at the lowest possible B_0 was found at B_0 = 2.3 T. The plasma density should be chosen at the lowest possible level providing reasonable efficiency of the ECRH and preventing the ECRH-induced generation of runaway electrons. The compromise was found at the line-averaged density $\bar{n}_e = 1.0\times10^{19}$ m^{-3} in the plasma discharges with I_{pl} = 230 kA.

The discharges under study contained up to four stages, differing in the level of ECRH power P_{EC} and localization of the EC-resonance zone in the plasma:
{1} – ohmic discharge, OH;
{2} – on-axis EC-heating (0.5 MW), gyrotron B;
{3} – off-axis EC heating (1.7 MW), gyrotrons A+C;
{4} – combined EC heating (2.2 MW), gyrotrons A+B+C.
The evolution of the main parameters of the discharges is shown in Fig. 2.

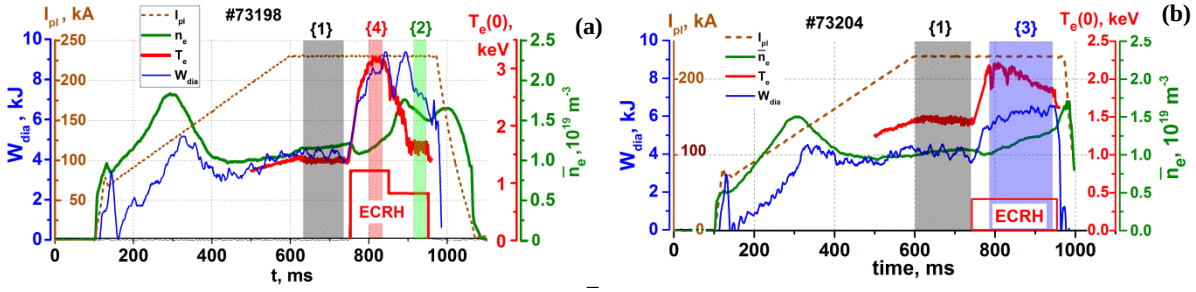

FIG. 2. Time evolution of current I_{pl}, line averaged density $\bar{n}_e$, central electron temperature $T_e(0)$ and stored energy W_{dia} in discharge with powerful combined ECRH. (a) scenario with P_{EC} = 0.5 MW, 2.2 MW, (b) scenario with P_{EC} = 1.7 MW.

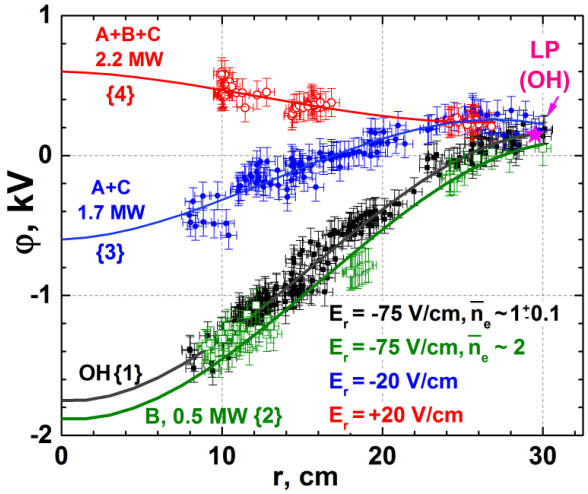

FIG. 3. Profiles of potential in the Ohmic phase (OH) and with switch on various groups of gyrotons A, B and C

3.1. Evolution of the mean plasma potential

Low-density OH deuterium plasmas ($\bar{n}_e = 1.0\times10^{19}$ m^{-3}, $T_e < 1.3$ keV, $T_i < 0.6$ keV) in T-10 are characterized by a negative potential up to $\varphi = -1500$ V near the centre ($\rho = 0.3$), Fig. 3. The potential profile is monotonically increasing towards the periphery, reaching the value of +100 V at the edge ($\rho = 1.0$) and forming the radially averaged electric field E_r = -75 V/cm. A density (collisionality) rise due to gas puff is accompanied by an increasing of the absolute value of negative potential. This is valid for the steady-state phase of the discharge, as for the initial phase of the plasma current and density ramp [9]. Powerful off-axis ($\rho_{EC} = 0.5$) second harmonic X-mode ECRH with $P_{EC\_off} \le 1.7$ MW ($f_{EC}^{off} = 144$ GHz), see plasma scenario in Fig. 2 (b), leads to an increase of T_e up to 2 keV in the centre, as measured by 2-ω ECE-diagnostics and shown in Fig. 4(a). In such low-density plasmas the incomplete absorption of EC waves is possible [10].

Also powerful ECRH leads to some decrease of the ion temperature, Fig. 4(b), and density pump-out, Fig. 4(c). The ECR heating is accompanied by decrease of the energy confinement time from 14 ms in OH, stage {1} to 3.5 ms at maximal P_{EC}, stage {4}. Potential profile has a sort of a plateau near the edge ($\rho = 0.8$-1.0). In the phase {4}), an extra nearly on-axis ($\rho = 0.2$) ECRH with $P_{EC}^{on} \le 0.5$ MW ($f_{EC}^{on} = 129$ GHz) leads to a further increase of $T_e(0)$ up to 3.3 keV and to an increase in the core plasma potential leading to φ = +500 V near the centre and a positive $E_r \sim +20$ V/cm from the plasma core to the edge as presented in Fig. 4. This is the first observation of the positive electric potential (electric field) in a core of tokamak plasma.

3.2. Evolution of the plasma turbulence

Plasma potential and density were measured simultaneously in 5 Sample volumes shown in Fig. 1. Let θ_{ij} is a phase shift between density signals measured in slits i, j, and dx_{ij} is a poloidal distance between slits i, j of the analyzer. The velocity of poloidal rotation of the density oscillations with frequency f is $V_f = dx_{ij}\, 2\,\pi\, f\, /\theta_{ij}$. If θ_{ij} is proportional to f in some frequency region, one may conclude the turbulence rotation as a whole in that frequency region with turbulence velocity V_{turb}. Figure 5 shows the density cross-phase θ_{ij} vs frequency for OH {1} and ABC {4} stages of the shot with changes of the potential sign. In the ohmic stage (black curve), a linear dependence of the phase on frequency starting from the origin is observed in the frequency range of 0–25 kHz.

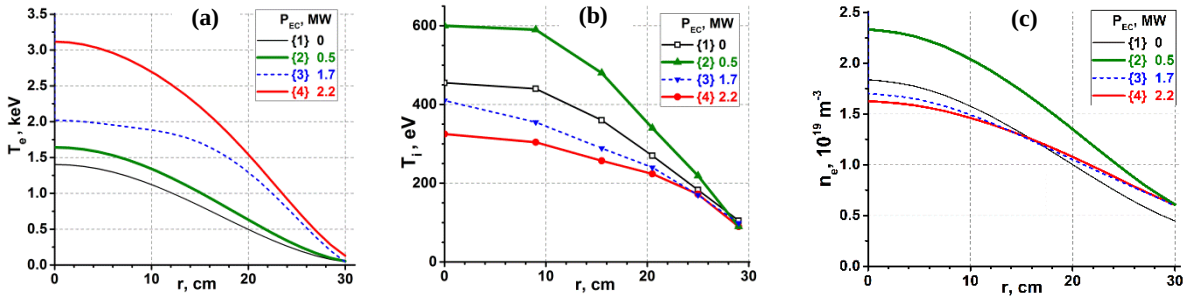

FIG. 4. Profiles of electron temperature (a), ion temperature (b) and density (c) at different ECRH power P_{EC}.

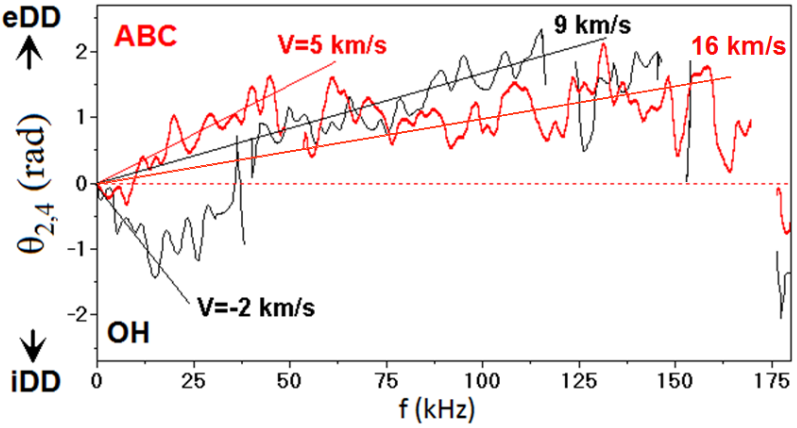

FIG. 5. The cross-phase of density fluctuations vs frequency for OH (black curve) and ABC (red curve) stages of the shot with changes of the potential sign #73197; B_t = 2.3 T, I_{pl} = 230 κA, E_b = 320 keV, r_{HIBP} = 0.09-0.11 m. The slope of straight lines allows to estimate the velocity of turbulence propagation for specified spectral range.

This is the frequency range of stochastic low-frequency (SLF) mode [11]. The linear dependence θ(*f*) can be interpreted as a poloidal rotation of low-frequency turbulence (SLF) in the ion-diamagnetic drift (iDD) direction with linear velocity $V_{SLF} \approx$ -2 km/s in the laboratory frame.

At the same time, at frequencies exceeding 40 kHz, the phase has opposite sign, showing electron-diamagnetic drift (eDD) direction, opposite to SLF [12]. This is the frequency range of quasi-coherent mode (QCM) [13], which is rotating with $V_{QCM} \approx$ +9 km/s. In between SLF and QCM there is an intermediate frequency area 25-40 kHz, where rotation is undetermined. The similar behaviour of the SLF and QCM opposite rotation was observed for higher density (collisionality) OH plasmas [14]. During powerful ECRH (ABC), the character of the θ(*f*) dependence changes significantly: the SLF changes the direction of rotation to eDD direction. For $f < 50$ kHz, SLF, the rotation velocity $V_{SLF} \approx$ +5 km/s. For higher frequencies, in the QCM frequency range, θ(*f*) slope shows an increase of the QCM velocity up to $V_{QCM} \approx$ +16 km/s. So, the whole observed frequency region, including SLF, intermediate frequency area 50-75 kHz and QCM, propagates to eDD direction.

HIBP measurements show that the density turbulence strongly changed with powerful ECRH, scenario {3}, Fig. 6: the lower frequencies, SLF and higher frequencies up to $f < 100$ kHz, present the increase of the oscillation power, while the QCM, dominating in the OH plasmas [14], became masked, as presented in Fig. 6 (b). The total RMS of the density fluctuation increases with ECRH power application, as presented in the Fig. 6 (c). Its maximal value increases up to a factor of 2 for P_{EC} =1.7 MW. Figure 7 shows the RMS of the core plasma density. We see that RMS increases up to a factor 2 of in the core area. The RMS of plasma potential shows an increase with a factor of 1.2.

4. DISCUSSION

The radial electric field can be found from plasma parameters using the radial force balance equation (see for example Eq. (1.2) in [1]):

$$E_r = (Z_i e n_i)^{-1} \nabla p_i - V_p B_t + V_t B_p \qquad (1)$$

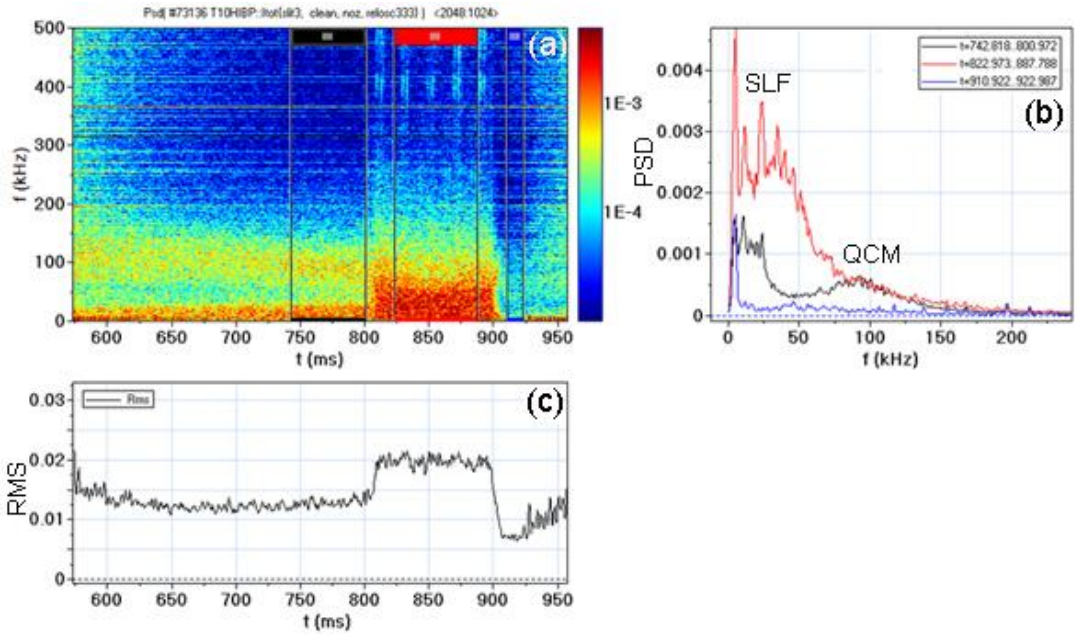

FIG. 6. Plasma density turbulence evolution in the shot #73136 with scenarios {1, 3}, P_{EC} < 1.7 MW. (a) Power spectrogram of the density fluctuations, (b) power spectra in OH (blue and black) and ECRH (red) phases of the discharge, (c) time trace of the density RMS; r_{HIBP}=0.12 m.

The first 'diamagnetic' term of this equation is always negative due to the negative sign of the ion pressure gradient ∇p_i. So, in absence of plasma rotation, E_r is always negative. In OH plasmas (stage {1}), spectroscopic CXRS measurements of the toroidal plasma rotation velocity V_t show the positive (counter to plasma current) direction, which is consistent with the negative plasma potential (electric field) due to the negative sign of poloidal magnetic field B_p. In the ECRH plasmas, experimental uncertainty in CXRS is much larger, nevertheless, the outcome is basically the same: the negative contribution to core E_r due to toroidal plasma rotation V_t. Neoclassical estimation of the poloidal rotation velocity, which is proportional to the ion temperature gradient, gives the negative contribution to the plasma potential (electric field). So, the obtained positive electric field is not consistent with NC approach.

Now we discuss the neoclassical approach to plasma rotation. We used Eq. (23) from [16] for E_r calculation, in which, along with the parallel viscosity $\Pi_{V\|}$, the terms with nonlinear convection of the longitudinal ion velocity $V_\| = V_t$ are taken into account. The solution to this equation with the boundary condition $E_r(r=a) = E_w = -(\lambda/e)\,dT_e(r=a)/dr$ has the form:

$$E_r(r) = \frac{T_i}{e}\left[\frac{n_e'}{n_e} + (1-k_{\rm NC})\frac{T_i'}{T_i}\right] + E_{\rm turb}\,, \qquad (2)$$

where $E_{\rm turb} = -\dfrac{B\varepsilon}{cq} n_e \dfrac{\Pi_{V\|}}{\Gamma_r} + E_w \dfrac{\Gamma_w}{\Gamma_r}$, $\lambda = {\rm const} \approx 3$, $\Gamma_r = \left\langle \tilde{n}_e \cdot \tilde{V}_r \right\rangle$ and $\Pi_{V\|} = \left\langle \tilde{V}_\| \cdot \tilde{V}_r \right\rangle$ are the turbulent particle and parallel momentum fluxes. Analytical expression for $k_{\rm NC}(\nu_{i*})$, where $\nu_{i*} = qR\,\nu_{ii}/\varepsilon^{3/2}\,V_{ti}$, $\varepsilon = r/R$, and V_{ti} is the thermal velocity of ions, is presented in [17].

Qualitative analysis of Eq. (2) shows that the first term makes a decisive (negative) contribution in the case of weak turbulence $\Pi_{V\|} << 1$; wherein $E_r < 0$ and it is close to NC value. The electric field $E_{\rm turb}$ driven by the turbulent transport of parallel momentum will be positive, if $dV_\|/dr > 0$, since then $\Pi_{V\|} = -\eta_{\rm turb}\, dV_\|/dr < 0$, where $\eta_{\rm turb}$ is the turbulent viscosity. Thus, in the case of strong turbulence (when $dV_\|/dr > 0$) the term ~ $\Pi_{V\|} < 0$ is dominated and $E_r > 0$. The third term input a small positive contribution $\left(dT_e(a)/dr < 0\right)$. With growth of T_e during ECR heating, the level of turbulent fluctuations increases (see Fig. 6) that due to the Reynolds stress $\left\langle \tilde{V}_\| \cdot \tilde{V}_r \right\rangle$ leads to growth of $E_{\rm turb} > 0$. The density pump-out leads to drop in the turbulent particle flow $\left\langle \tilde{n} \cdot \tilde{V}_r \right\rangle$ that also leads to growth of $E_{\rm turb} > 0$. In contrast to NC, the turbulence may give the positive contribution to the electric field $E_{\rm turb}$.

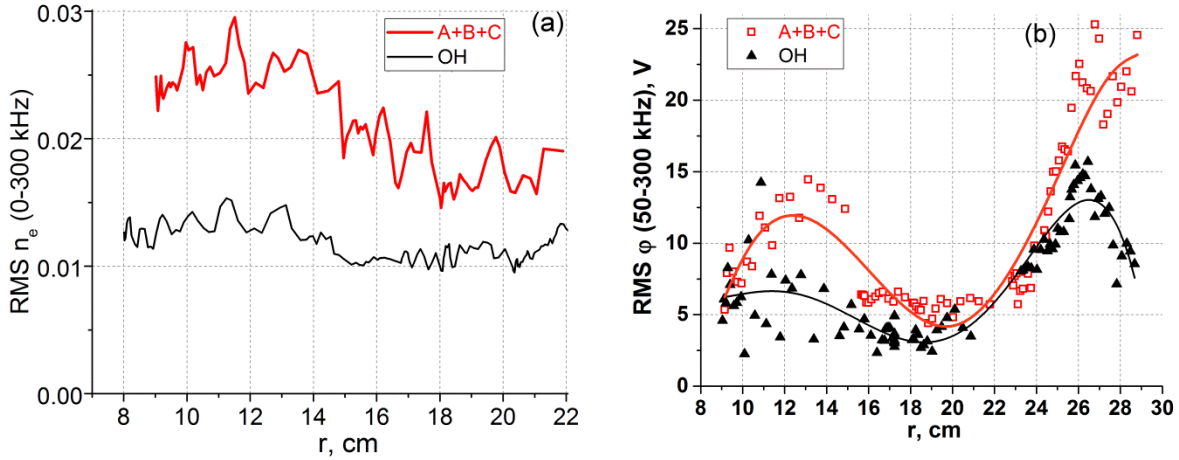

FIG. 7. The radial distribution of RMS for density (a) and potential (b) turbulence in OH {1} and powerful ECR heating {4} stages.

TABLE 1. COMPARISON OF COLLISIONALITIES IN T-10 AND ITER

Regime, gyrotrons	$\bar{n}_e$ (10^{19} m^{-3})	$T_e(0)$ (keV)	Z_{eff}	ν_{eff}	φ_0 (kV)
T-10 {1}, OH	1.17	1.4	2.5	0.224	-1.75
T-10 {2}, B	1.6	1.75	2.1	0.165	-1.85
T-10 {3}, AC	1.2	2	2.5	0.113	-0.6
T-10 {4}, ABC	1.2	3.2	3	0.053	0.6
ITER L-mode	6.2	8	1.8	0.105	
ITER H-mode Burn	8.9	23.5	1.8	0.017	

Finally, the observed plasma electrostatic (density and potential) turbulence increase in the low-density ECRH plasmas is consistent with mean plasma potential evolution from negative to positive values due to the turbulence contribution E_{turb}.

The earlier studies of plasma potential on T-10 have shown that core negative plasma potential tends to decrease in absolute value with decrease of collisionality ν_{eff} [18], where $\nu_{eff} = 0.1 \cdot R \cdot Z_{eff} \cdot n_e/T_e(0)^2$ [19]. The parameters of the discharges under study altogether with the ITER baseline scenario, taken from [20] are presented in TABLE 1. The core plasma potential versus collisionality is shown in Fig. 8. Ohmic phase of the discharges under analysis are characterized by reasonably low ν_{eff} due to the low density relatively to the "standard" T-10 tokamak discharge, having $\bar{n}_e \sim 2.0 - 4.0 \times 10^{19}$ m^{-3}. Auxiliary ECRH causes a further decrease of ν_{eff} due to high electron temperature T_e towards the so-called 'banana' collisional regime, which is expected to be an operational regime for the future fusion reactors.

It was shown earlier that the core potential in tokamak plasmas were always negative [21–26], in contrast to stellarators, where it was either negative or positive depending on plasma conditions. The present T-10 results compares remarkably well with the positive plasma potential obtained in the TJ-II stellarator with powerful ($P_{EC\text{-}on} \leq 0.6$ MW) second harmonic X-mode ECRH [4] for plasmas with similar dimensions and parameters as in T-10. The same is valid for other stellarators like CHS [3] and LHD [27], where the positive potential was observed for low-density (low-collisionality) ECRH plasmas. Obtaining the positive potential in a tokamak fills the existed gap and completes the picture (general observations): the higher is the plasma collisionality, the higher is the negative potential in toroidal plasmas; the lower is the plasma collisionality the higher is the positive potential in toroidal plasmas. (Note that above some collisionality limit, the negative potential saturates). Therefore, the obtained low-collisionality regime with positive potential in the core plasmas allows us to predict the positive plasma potential in the future fusion plasma reactor like ITER. The same holds for fusion reactor based on the stellarator concept.

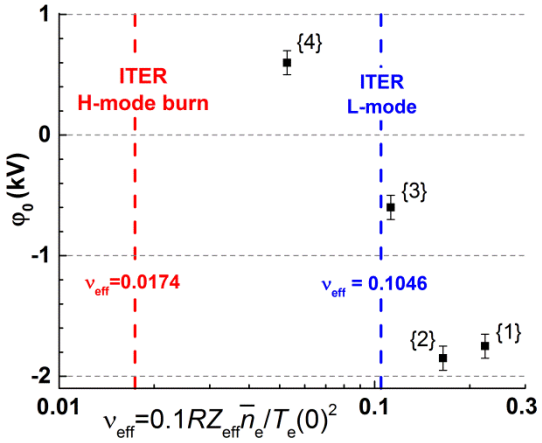

FIG. 8. The plasma potential vs collisionality in T-10 regimes with OH and ECRH, and estimations for ITER.

5. SUMMARY

The first observation of the positive electric potential φ = +500 V near the centre and a positive electric field E_r ~ +20 V/cm in a core tokamak plasma was done. This observation is consistent not with NC expectations, rather with turbulence effects, that is supported by an increase of the electrostatic fluctuations with powerful ECRH. The coupling of core plasma potential and collisionality experimentally established in a wide range of plasma parameters was extended to the low-collisionality plasmas. Based on that, the positive plasma potential is predicted for ITER collisionless plasmas.

ACKNOWLEDGEMENTS

The study was supported by Russian Science Foundation, Project 19-12-00312. AVM was partly supported by Competitiveness program of NRNU MEPhI.

REFERENCES

[1] MELNIKOV, A.V., Electric Potential in Toroidal Plasmas, Springer Nature Switzerland AG (2019).
[2] GALEEV, A.A. and SAGDEEV, R.Z. Sov. Phys. JETP **26** (1968) 233.
[3] FUJISAWA, A., IGUCHI, H., SANUKI, H. et al., Dynamic behavior of potential in the plasma core of the CHS heliotron/torsatron, Phys. Rev. Lett. **79** (1997) 1054-1057.
[4] MELNIKOV, A.V., ALONSO, A., ASCASIBAR, E., et al., Plasma potential evolution study by HIBP diagnostic during experiments in the TJ-II stellarator, Fusion Sci. Technol. **51** (2007) 31-37.
[5] SHIMIZU, A., IDO, T., KURACHI, M., et al., 2D potential measurements by applying automatic beam adjustment system to heavy ion beam probe diagnostic on the Large Helical Device, Rev. Sci. Instrum. **85** (2014) 11D853.
[6] MELNIKOV, A.V., Applied and fundamental aspects of fusion science, Nature Phys. **12** (2016) 386-390.
[7] DRABINSKIY, M.A., Technical aspects of the heavy ion beam probing design and operation at the T-10 tokamak, J. Phys.: Conf. Series, **1147** (2019) 012123.
[8] MELNIKOV, A.V., DRABINSKIY, M.A., ELISEEV, L.G., et al., Heavy ion beam probe design and operation on the T-10 tokamak, Fusion Eng. Design **146**, Part A (2019) 850-853.
[9] MELNIKOV, A.V., HIDALGO, C., ELISEEV, L.G., et al., Plasma potential and turbulence dynamics in toroidal devices (survey of T-10 and TJ-II experiments), Nucl. Fusion **51** (2011) 083043.
[10] DNESTROVSKIJ, Y.N., DANILOV, A.V., DNESTROVSKIJ A.Y., et al., Transport model of plasma heating at the second harmonic of the electron cyclotron frequency, Plasma Phys. Control. Fusion **63** (2021) 055012.
[11] VERSHKOV, V.A., SHELUKHIN, D.A., SOLDATOV, S.V., et al., Summary of experimental core turbulence characteristics in ohmic and electron cyclotron resonance heated discharges in T-10 tokamak plasmas, Nucl. Fusion **45** (2005) S203-S226.
[12] VERSHKOV, V.A., BULDAKOV, M.A., SUBBOTIN, G.F., et al., 3D structure of density fluctuations in the T-10 tokamak and new approach for current profile estimation, Nucl. Fusion **59** (2019) 066021.

[13] VERSHKOV, V.A., SHELUKHIN, D.A., SUBBOTIN, G.F., et al., Density fluctuations as an intrinsic mechanism of pressure profile formation, Nucl. Fusion **55** (2015) 063014.
[14] MELNIKOV, A.V., et al., "Studies of poloidal rotation of plasma density turbulence with HIBP in the T-10 tokamak". Proc. 46th EPS Conf. on Plasma Physics, Milano, 8-12 July 2019, ECA, vol. 43C, Rep. P5.1090.
[15] ELISEEV, L.G., MELNIKOV, A.V., LYSENKO, S.E., et al., Evaluation of turbulent particle flux by heavy ion beam probe in the T-10 tokamak, Plasma Fusion Research **13** (2018) 3402106.
[16] ROZHANSKY, V., KAVEEVA, E., VOSKOBOYNIKOV, S., et al., Radial electric field in the biasing experiments and effective conductivity in a tokamak, Phys. Plasmas **9** (2002) 3385-3394.
[17] KIM, Y.B., DIAMOND, P.H. and GROENBER, R.J., Neoclassical poloidal and toroidal rotation in tokamaks, Phys. Fluids B **3** (1991) 2050-2060.
[18] MELNIKOV, A.V., ELISEEV, L.G., PERFILOV, S.V., et al., Electric potential dynamics in OH and ECRH plasmas in the T-10 tokamak, Nucl. Fusion **53** (2013) 093019.
[19] ANGIONI, C., PEETERS, A.G., GARBET, X., et al., Density response to central electron heating: theoretical investigations and experimental observations in ASDEX Upgrade, Nucl. Fusion **44** (2004) 827.
[20] CASPER, T., GRIBOV, Y., KAVIN, A., et al., Development of the ITER baseline inductive scenario, Nucl. Fusion **54** (2014) 013005.
[21] HOSEA, J., JOBES, F.C., HICKOK, R.L., et al., Rotation and structure of low-frequency oscillations inside the ST-tokamak plasma, Phys. Rev. Lett. **30** (1973) 839-842.
[22] BUGARYA, V.I., GORSHKOV, A.V., GRASHIN, S.A., et al. Measurements of plasma column rotation and potential in the TM-4 tokamak, Nucl. Fusion **25** (1985) 1707-1717.
[23] YANG, X.Z., ZHANG, B.Z., WOOTTON, A.J., et al. The space potential in the tokamak TEXT, Phys. Fluids B **3** (1991) 3448-3461.
[24] HAMADA, Y., NISHIZAWA, A., KAWASUMI, Y., et al., Measurement of profiles of the space potential in JIPP T-IIU tokamak plasmas by slow poloidal and fast toroidal sweeps of a heavy ion beam, Plasma Phys. Control. Fusion **36** (1994) 1743-1762.
[25] IDO, T., KAMIYA, K., MIURA, Y., et al., Observation of the fast potential change at L-H transition by a heavy-ion-beam probe on JFT-2M, Phys. Rev. Lett. **88** (2002) 055006.
[26] MELNIKOV, A.V., HIDALGO, C., IDO, T., et al., Plasma potential in toroidal devices: T-10, TJ-II, CHS and LHD, Plasma Fusion Res. **7** (2012) 2402114.
[27] SHIMIZU, A., IDO, T., NISHIURA, M., et. al., Development of 2D potential profile measurements using the heavy ion beam probe on the large helical device, Plasma Fusion Res. **11** (2016) 2402123.